Acta Mechanica Solida Sinica, Vol. 31, No. 3, June, 2018
https://doi.org/10.1007/s10338-018-0015-9
ISSN 1860-2134

Elastic Wave Scattering and Dynamic Stress Concentrations in Stretching Thick Plates with Two Cutouts by Using the Refined Dynamic Theory

Chuan-ping Zhou[1,2] **Qiao-yi Wang**[1⋆] **Denghao Chen**[1] **Chao Hu**[3]
Ban Wang[1] **Fai Ma**[4]

([1] *Zhejiang Key Laboratory of Mechanical Equipment and Technology for Marine Machinery, School of Mechanical Engineering, Hangzhou Dianzi University, Hangzhou 300018, China*)
([2] *School of Mechatronic Engineering, China University of Mining and Technology, Xuzhou 221116, China*)
([3] *School of Aerospace Engineering and Applied Mechanics, Tongji University, Shanghai 200092, China*)
([4] *College of Engineering, University of California, Berkeley, CA 94720, USA*)

Received 10 July 2017; revision received 29 September 2017; Accepted 7 January 2018;
published online 31 March 2018

ABSTRACT Based on the refined dynamic equation of stretching plates, the elastic tension–compression wave scattering and dynamic stress concentrations in the thick plate with two cutouts are studied. In view of the problem that the shear stress is automatically satisfied under the free boundary condition, the generalized stress of the first-order vanishing moment of shear stress is considered. The numerical results indicate that, as the cutout is thick, the maximum value of the dynamic stress factor obtained using the refined dynamic theory is 19% higher than that from the solution of plane stress problems of elastic dynamics.

KEY WORDS Refined vibration equation of stretching plate, Thick plate, First moment of shear stress, Elastic wave scattering, Dynamic stress concentration

1. Introduction

As typical structures, plates are widely used in aerospace industry, civil and construction engineering, and mechanical engineering. It is inevitable to make cutouts in the plates to meet the engineering design requirements. The cutouts reduce the loading capacity and life time of the structure. Therefore, many experts and scholars studied the problems on static and dynamic stress concentration around the cutouts [1–6]. The elastic wave methods can be used to describe and simulate the stress–strain states which are produced by a variety of dynamic loads in solid media or structures [7, 8]. The elastic wave propagation, scattering and dynamic stress concentration, as well as localization of vibration in a plate with cutouts are important frontier problems in the realm of mechanics. The investigations on these problems can promote the innovation and development of classical structural dynamics and the problem-solving methods.

In the past, the solution of plane elasticity problem [5, 7], instead of the solution for stretching plates, was often used to investigate stress concentrations for engineering design, for instance, the Kirsch solution [9] of the elasticity problem and the plane stress problem on elastic dynamics. However,

⋆ Corresponding author. E-mail: wangqiaoyi1966@hotmail.com

the plane stress solution is formulated in terms of the average stresses and average displacements across the thickness of plate, not in terms of the pertinent values at each field point [3]. Thus, it may lead to erroneous result when the displacements vary sharply across the thickness. Such is the case when the plate vibrates longitudinally at high frequencies. A comparison [10] with the results based on the three-dimensional theory of elasticity shows that the generalized plane stress approximation for a plate is valid only when the frequency is low and the wavelength is large. It is evident that the two-dimensional model is very different from the actual structure in solving the stress concentration problems. For these reasons, establishing exact thick-walled stretching plate models is needed for solving the problems of stress concentration in structures. Many scholars proposed refined theories [11–13] to reduce engineering errors.

Although those refined theories have been modified and optimized plane stress theories, in essence they were based on geometric approaches, and the models were coarse since engineering assumptions were still used during the derivation, resulting in many limitations in the application of thick-walled structure, especially in case of plates vibrating at higher frequencies. In this paper, based on not the geometric view but the algebraic view [14–16], we propose a novel exact elastodynamics theory for stretching plates. During the derivation, we apply the general solution proposed by Boussinesq–Galerkin and the operator theory of partial differential equations. The refined elastodynamics equations for stretching plates are obtained by applying appropriate gauge conditions. Then, based on the obtained refined theory, elastic wave scattering and dynamic stress concentrations in plates with two cutouts are studied. As examples, the dynamic stress concentration factors in stretching plates with two circular cutouts are numerically computed and analyzed with different parameters. Since the dynamic equation is derived without any prior assumptions, the proposed dynamic equation of plate is more exact and can be applied in a wider frequency range and greater thickness.

2. Derivation of the Refined Plate Theory for Elastodynamics of Thick Plate

Consider an infinite thick plate subjected to elastic tension–compression waves, as depicted in Fig. 1. Two circular cutouts of radius a are buried in the plate. First, we introduce the derivation process of the refined plate theory for elastodynamics of thick plate. According to the three-dimensional elastodynamics theory, the governing equation of the spatial displacement field is the Navier equation as

$$\mu\nabla_0^2\boldsymbol{u} + (\lambda+\mu)\,\nabla_0\,(\nabla_0\cdot\boldsymbol{u}) = \rho\frac{\partial^2\boldsymbol{u}}{\partial t^2} \tag{1}$$

where μ, λ are the Lame constants, $\lambda = \frac{\nu E_{\mathrm{M}}}{(1+\nu)(1-2\nu)}$, and $\mu = \frac{E_{\mathrm{M}}}{2(1+\nu)}$, in which E_{M} is elastic modulus, ν is Poisson's ratio, ρ is density, and t is time; and $\nabla_0 = \boldsymbol{e}_1\frac{\partial}{\partial x} + \boldsymbol{e}_2\frac{\partial}{\partial y} + \boldsymbol{e}_3\frac{\partial}{\partial z}$ is the three-dimensional

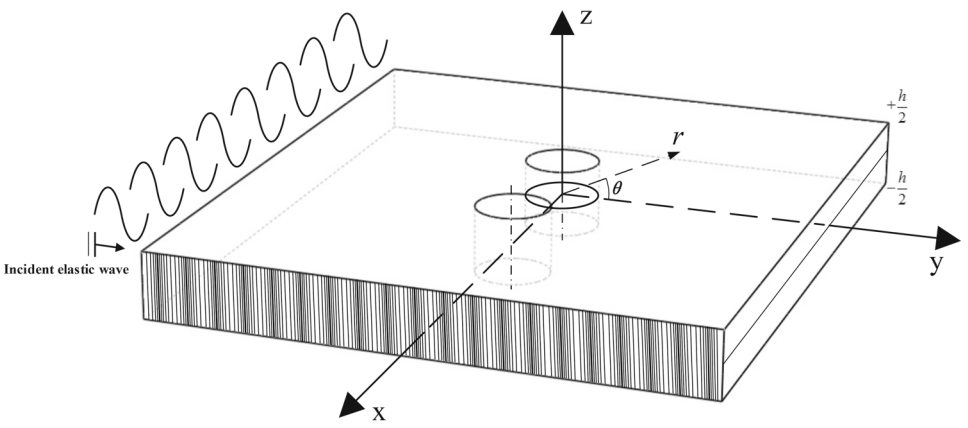

Fig. 1. Sketch of tension–compression elastic waves incident upon a thick plate with two cutouts

Hamilton operator, whose corresponding Laplace operator can be written as $\nabla_0^2 = \frac{\partial^2}{\partial x^2} + \frac{\partial^2}{\partial y^2} + \frac{\partial^2}{\partial z^2} = \nabla^2 + \frac{\partial^2}{\partial z^2}$.

The elastodynamics solution of Eq. (1) given by Boussinesq–Galerkin (the B–G solution) is

$$\boldsymbol{u} = 2(1-\nu)\left(\nabla_0^2 - T_j^2\right)\boldsymbol{G} - \nabla_0\left(\nabla_0 \cdot \boldsymbol{G}\right) \tag{2}$$

where $T_j^2 = \frac{1}{c_j^2}\frac{\partial^2}{\partial t^2}$ $(j = 1, 2)$, with c_1, c_2 being the longitudinal and transverse wave velocities, respectively, $c_1^2 = \frac{\lambda+2\mu}{\rho}$, and $c_2^2 = \frac{\mu}{\rho}$; and $\boldsymbol{G} = G_1\boldsymbol{e}_1 + G_2\boldsymbol{e}_2 + G_3\boldsymbol{e}_3$ is the Somigliana vector potential function which satisfies

$$\prod_{j=1}^{2}\left(\nabla_0^2 - T_j^2\right)G = 0 \tag{3}$$

Here, we use numbers 1, 2, 3 to denote the coordinates x, y, z, respectively. According to the Taylor series expansion, by using the exponential function operator, the displacement of any point in the plate can be described as

$$u_k(x, y, z, t) = \exp\left(z\frac{\partial}{\partial z}\right)u_k(x, y, 0, t) \quad (k = 1, 2, 3) \tag{4}$$

In order to simplify the analysis, we introduce the concept of virtual differential operator, where $\mathrm{i}\square_j = \sqrt{T_j^2 - \nabla^2}$ for extending algebraic analysis and spectral theory of partial differential equations.

According to Eqs. (2) and (4), we can obtain

$$\begin{aligned} G_k(x, y, z, t) &= \exp\left(z\frac{\partial}{\partial z}\right)G_k(x, y, 0, t) \\ &= \exp\left(z\frac{\partial}{\partial z}\right)\sum_{j=1}^{2}G_k^j(x, y, 0, t) \\ &= 2\mathrm{Re}\left[\sum_{j=1}^{2}\exp(z\mathrm{i}\square_j)g_k^{j1}\right] \end{aligned} \tag{5}$$

where $\mathrm{Re}(\cdot)$ denotes computation of the real part, $\square_j^2 = \nabla^2 - T_j^2$ $(j = 1, 2)$ is the Lorentz operator, $\mathrm{i}\square_j$ is the virtual differential operator, $\boldsymbol{G} = \boldsymbol{G}^1 + \boldsymbol{G}^2$, $G^j = G^{j1} + G^{j2}$, $\left(\square_j^2 + \frac{\partial^2}{\partial z^2}\right)G^j = 0$, $\left(\frac{\partial}{\partial z} - \mathrm{i}\square_j\right)G^{j1} = 0$, and $\left(\frac{\partial}{\partial z} + \mathrm{i}\square_j\right)G^{j2} = 0$, with $j = 1, 2$.

And we can also obtain

$$\begin{aligned} \nabla_0 \cdot \boldsymbol{G} &= \frac{\partial G_1}{\partial x} + \frac{\partial G_2}{\partial y} + \frac{\partial G_3}{\partial z} \\ &= 2\mathrm{Re}\left[\sum_{j=1}^{2}\exp(\mathrm{i}z\square_j)\left(\frac{\partial}{\partial x}g_1^{j1} + \frac{\partial}{\partial y}g_2^{j1} + \mathrm{i}\square_j g_3^{j1}\right)\right] \end{aligned} \tag{6}$$

In order to eliminate the non-uniqueness of the unknown functions, the following two gauge conditions are applied:

$$\nabla \cdot \boldsymbol{g}^{11} = 0, \quad \nabla \cdot \boldsymbol{g}^{21} = 0 \tag{7}$$

where $\boldsymbol{g}^{ji} = g_1^{ji}\boldsymbol{e}_1 + g_2^{ji}\boldsymbol{e}_2$, $(i = 1, 2; j = 1, 2)$. It should be noted that g_k^{ji} $(k = 1, 2)$ is a complex function.

The following equation can be derived from Eqs. (7) and (8) as

$$\begin{aligned}\nabla_0(\nabla_0\cdot\boldsymbol{G}) = &-2\mathrm{Im}\left[\sum_{j=1}^{2}\exp(\mathrm{i}z\square_j)\,\square_j\frac{\partial g_3^{j1}}{\partial x}\right]\boldsymbol{e}_1\\ &-2\mathrm{Im}\left[\sum_{j=1}^{2}\exp(\mathrm{i}z\square_j)\,\square_j\frac{\partial g_3^{j1}}{\partial y}\right]\boldsymbol{e}_2\\ &-2\mathrm{Re}\left[\sum_{j=1}^{2}\exp(\mathrm{i}z\square_j)\,\square_j^2 g_3^{j1}\right]\boldsymbol{e}_3\end{aligned}\tag{8}$$

in which $\mathrm{Im}(\cdot)$ denotes computation of the imaginary part.

According to Eq. (2), the vibration displacement in the plate can be expressed as

$$u_k = 2\mathrm{Re}\left[\exp(iz\square_2)T_2^2 g_k^{21}\right] + 2\mathrm{Im}\left[\sum_{j=1}^{2}\exp(\mathrm{i}z\square_j)\square_j\frac{\partial}{\partial x_k}g_3^{j1}\right]\qquad(k=1,2)\tag{9a}$$

$$u_3 = 2\mathrm{Re}\left[\exp(\mathrm{i}z\square_2)T_2^2 g_3^{21}\right] + 2\mathrm{Re}\left[\sum_{j=1}^{2}\exp(\mathrm{i}z\square_j)\square_j^2 g_3^{j1}\right]\tag{9b}$$

The neutral surface displacement, normal rotation angle, and transverse normal strain in the plate can be expressed as

$$\begin{aligned}U_k &= u_k|_{z=0} = 2\mathrm{Re}\left(T_2^2 g_k^{21}\right) + 2\mathrm{Im}\left(\sum_{j=1}^{2}\square_j\frac{\partial}{\partial x_k}g_3^{j1}\right)\quad(k=1,2)\\ W &= u_z|_{z=0} = 2\mathrm{Re}\left(T_2^2 g_3^{21}\right) + 2\mathrm{Re}\left(\sum_{j=1}^{2}\square_j^2 g_3^{j1}\right)\\ \psi_k &= -\frac{\partial u_k}{\partial z}|_{z=0} = 2\mathrm{Im}\left(\square_2 T_2^2 g_k^{21}\right) - 2\mathrm{Re}\left(\sum_{j=1}^{2}\square_j^2\frac{\partial}{\partial x_k}g_3^{j1}\right)\quad(k=1,2)\\ E &= \frac{\partial u_k}{\partial z}|_{z=0} = -2\mathrm{Im}\left(\square_2 T_2^2 g_3^{21}\right) - 2\mathrm{Im}\left(\sum_{j=1}^{2}\square_j^3 g_3^{j1}\right)\end{aligned}\tag{10}$$

Considering the decomposition method for the neutral surface angle and displacement function as follows,

$$\begin{aligned}\psi_1 &= \frac{\partial}{\partial x}F^{(1)} + \frac{\partial}{\partial y}f^{(1)}, \qquad \psi_2 = \frac{\partial}{\partial y}F^{(1)} - \frac{\partial}{\partial x}f^{(1)}\\ U_1 &= \frac{\partial}{\partial x}F^{(2)} + \frac{\partial}{\partial y}f^{(2)}, \qquad U_2 = \frac{\partial}{\partial y}F^{(2)} - \frac{\partial}{\partial x}f^{(2)}\end{aligned}\tag{11}$$

the following relations can be obtained by the derivation and the calculus as

$$\begin{aligned}\mathrm{Im}\left(g_1^{21}\right) &= \frac{1}{2}\square_2^{-1}T_2^{-2}\frac{\partial}{\partial y}f^{(1)},\\ \mathrm{Im}\left(g_2^{21}\right) &= -\frac{1}{2}\square_2^{-1}T_2^{-2}\frac{\partial}{\partial x}f^{(1)}\\ \mathrm{Re}\left(g_1^{21}\right) &= \frac{1}{2}T_2^{-2}\frac{\partial}{\partial y}f^{(2)},\end{aligned}$$

$$
\begin{aligned}
&\mathrm{Re}\left(g_2^{21}\right) = -\frac{1}{2}T_2^{-2}\frac{\partial}{\partial x}f^{(2)}\\
&\mathrm{Re}\left(g_3^{11}\right) = -\frac{1}{2}\square_1^{-2}\left[F^{(1)} + \square_2^2 T_2^{-2}\left(W + F^{(1)}\right)\right]\\
&\mathrm{Re}\left(g_3^{21}\right) = \frac{1}{2}T_2^{-2}\left(W + F^{(1)}\right)\\
&\mathrm{Im}\left(g_3^{11}\right) = \frac{1}{2}\square_1^{-1}\left[T_1^{-2}\left(\square_1^2 F^{(2)} + E\right) + F^{(2)}\right]\\
&\mathrm{Im}\left(g_3^{21}\right) = -\frac{1}{2}T_1^{-2}\square_2^{-1}\left(\square_1^2 F^{(2)} + E\right)
\end{aligned}
\tag{12}
$$

where the negative exponent of the operator is the inverse of the differential operator, which can be expressed by the integral of the Green's function.

In this way, the total displacement of the bending and stretching vibration of the plate can be derived as

$$
\begin{aligned}
u_k = {} & 2T_2^2\left[\cos\left(z\square_2\right)\mathrm{Re}\left(g_k^{21}\right) - \sin\left(z\square_2\right)\mathrm{Im}\left(g_k^{21}\right)\right]\\
& + 2\sum_{j=1}^{2}\square_j\frac{\partial}{\partial x_k}\left[\cos\left(z\square_j\right)\mathrm{Im}\left(g_3^{j1}\right) + \sin\left(z\square_j\right)\mathrm{Re}\left(g_3^{j1}\right)\right] \quad (k=1,2)
\end{aligned}
\tag{13a}
$$

$$
\begin{aligned}
u_3 = {} & 2T_2^2\left[\cos\left(z\square_2\right)\mathrm{Re}\left(g_3^{21}\right) - \sin\left(z\square_2\right)\mathrm{Im}\left(g_3^{21}\right)\right]\\
& + 2\sum_{j=1}^{2}\square_j^2\left[\cos\left(z\square_j\right)\mathrm{Re}\left(g_3^{j1}\right) - \sin\left(z\square_j\right)\mathrm{Im}\left(g_3^{j1}\right)\right]
\end{aligned}
\tag{13b}
$$

According to the Hooke's law, the stress components can be written as

$$
\begin{aligned}
\tau_{zx} = \mu_{\mathrm{M}}\Bigg\{ & -2\square_2 T_2^2\left[\sin(z\square_2)\mathrm{Re}(g_1^{21}) + \cos(z\square_2)\mathrm{Im}\left(g_1^{21}\right)\right]\\
& - 4\sum_{j=1}^{2}\sin(z\square_j)\square_j^2\frac{\partial}{\partial x}\mathrm{Im}\left(g_3^{j1}\right) + 4\sum_{j=1}^{2}\cos(z\square_j)\square_j^2\frac{\partial}{\partial x}\mathrm{Re}\left(g_3^{j1}\right)\\
& + 2T_2^2\left[\cos(z\square_2)\frac{\partial}{\partial x}\mathrm{Re}\left(g_3^{21}\right) - \sin(z\square_2)\frac{\partial}{\partial x}\mathrm{Im}\left(g_3^{21}\right)\right]\Bigg\}
\end{aligned}
\tag{14a}
$$

$$
\begin{aligned}
\tau_{zy} = \mu_{\mathrm{M}}\Bigg\{ & -2\square_2 T_2^2\left[\sin(z\square_2)\mathrm{Re}\left(g_2^{21}\right) + \cos(z\square_2)\mathrm{Im}\left(g_2^{21}\right)\right]\\
& - 4\sum_{j=1}^{2}\sin(z\square_j)\square_j^2\frac{\partial}{\partial y}\mathrm{Im}\left(g_3^{j1}\right) + 4\sum_{j=1}^{2}\cos(z\square_j)\square_j^2\frac{\partial}{\partial y}\mathrm{Re}\left(g_3^{j1}\right)\\
& + 2T_2^2\left[\cos(z\square_2)\frac{\partial}{\partial y}\mathrm{Re}\left(g_3^{21}\right) - \sin(z\square_2)\frac{\partial}{\partial y}\mathrm{Im}\left(g_3^{21}\right)\right]\Bigg\}
\end{aligned}
\tag{14b}
$$

$$
\begin{aligned}
\sigma_z = {} & 2(\lambda+2\mu)\square_1 T_1^2\left[\cos(z\square_1)\mathrm{Im}\left(g_3^{11}\right) + \sin(z\square_1)\mathrm{Re}\left(g_3^{11}\right)\right]\\
& - 4\mu\sum_{j=1}^{2}\nabla^2\square_j\left[\cos(z\square_j)\mathrm{Im}\left(g_3^{j1}\right) + \sin(z\square_j)\mathrm{Re}\left(g_3^{j1}\right)\right]
\end{aligned}
\tag{14c}
$$

The load on the surface of a plate is divided into the symmetric and asymmetric parts. In line with the free boundary condition that the shear stress at the surface of a plate is zero and the normal stress, the following equations can be derived as

$$\frac{\partial}{\partial x}\left[2\cos\left(\frac{h}{2}\square_1\right)F^{(1)}+2\square_2^2T_2^{-2}\sum_{j=1}^{2}(-1)^{j-1}\cos\left(\frac{h}{2}\square_j\right)(W+F^{(1)})-\cos\left(\frac{h}{2}\square_2\right)(W+F^{(1)})\right]$$
$$\pm\frac{\partial}{\partial x}\left[2\square_1\sin\left(\frac{h}{2}\square_1\right)F^{(2)}+2T_1^{-2}\sum_{j=1}^{2}(-1)^{j-1}\square_j\sin\left(\frac{h}{2}\square_j\right)\left(\square_1^2F^{(2)}+E\right)-\frac{1}{\kappa}\frac{\sin\left(\frac{h}{2}\square_2\right)}{\square_2}\left(\square_1^2F^{(2)}+E\right)\right]$$
$$=\frac{\partial}{\partial x}\left[\cos\left(\frac{h}{2}\square_2\right)f^{(1)}\pm\square_2\sin\left(\frac{h}{2}\square_2\right)f^{(2)}\right] \tag{15a}$$

$$\frac{\partial}{\partial y}\left[2\cos\left(\frac{h}{2}\square_1\right)F^{(1)}+2\square_2^2T_2^{-2}\sum_{j=1}^{2}(-1)^{j-1}\cos\left(\frac{h}{2}\square_j\right)(W+F^{(1)})-\cos\left(\frac{h}{2}\square_2\right)(W+F^{(1)})\right]$$
$$\pm\frac{\partial}{\partial y}\left[2\square_1\sin\left(\frac{h}{2}\square_1\right)F^{(2)}+2T_1^{-2}\sum_{j=1}^{2}(-1)^{j-1}\square_j\sin\left(\frac{h}{2}\square_j\right)(\square_1^2F^{(2)}+E)\right.$$
$$\left.-\frac{1}{\kappa}\frac{\sin\left(\frac{h}{2}\square_2\right)}{\square_2}(\square_1^2F^{(2)}+E)\right]$$
$$=\frac{\partial}{\partial x}\left[\cos\left(\frac{h}{2}\square_2\right)f^{(1)}\pm\square_2\sin\left(\frac{h}{2}\square_2\right)f^{(2)}\right] \tag{15b}$$

$$(\lambda+2\mu)\left\{-\cos\left(\frac{h}{2}\square_1\right)\left[\left(\square_1^2F^{(2)}+E\right)+T_1^2F^{(2)}\right]\pm\frac{\sin\left(\frac{h}{2}\square_1\right)}{\square_1}\left[\kappa\square_2^2\left(W+F^{(1)}\right)+T_1^2F^{(1)}\right]\right\}$$
$$-2\mu\nabla^2\left[T_1^{-2}\sum_{j=1}^{2}(-1)^{j-1}\cos\left(\frac{h}{2}\square_j\right)\left(\square_1^2F^{(2)}+E\right)+\cos\left(\frac{h}{2}\square_1\right)F^{(2)}\right]$$
$$\pm2\mu\nabla^2\left[\sin\left(\frac{h}{2}\square_1\right)\square_1^{-1}F^{(1)}+\square_2^2T_2^{-2}\sum_{j=1}^{2}(-1)^{j-1}\frac{\sin\left(\frac{h}{2}\square_j\right)}{\square_j}\left(W+F^{(1)}\right)\right]=\pm\frac{1}{2}q+\frac{1}{2}q \tag{16}$$

where h is the thickness of the plate, and q is the transverse loads.

On the basis of the complex variable function theory, Eq. (15) can be regarded as a Riemann condition involving the real part and imaginary part of the analytic function, so there can be

$$2\cos\left(\frac{h}{2}\square_1\right)F^{(1)}+2\square_2^2T_2^{-2}\sum_{j=1}^{2}(-1)^{j-1}\cos\left(\frac{h}{2}\square_j\right)(W+F^{(1)})$$
$$-\cos\left(\frac{h}{2}\square_2\right)(W+F^{(1)})\pm\left[2\square_1\sin\left(\frac{h}{2}\square_1\right)F^{(2)}+2T_1^{-2}\sum_{j=1}^{2}(-1)^{j-1}\right.$$
$$\left.\times\square_j\sin\left(\frac{h}{2}\square_j\right)\left(\square_1^2F^{(2)}+E\right)-\frac{1}{\kappa}\frac{\sin\left(\frac{h}{2}\square_2\right)}{\square_2}(\square_1^2F^{(2)}+E)\right]=0 \tag{17a}$$

$$\cos\left(\frac{h}{2}\square_2\right)f^{(1)}\pm\square_2\sin\left(\frac{h}{2}\square_2\right)f^{(2)}=0 \tag{17b}$$

where $\kappa=\frac{c_2^2}{c_1^2}=\frac{1-2\nu}{2(1-\nu)}$.

The vibration of plate structure is decomposed into the symmetric and asymmetric motions. As we see, the bending vibration of plate is an asymmetric motion, and the stretching vibration of plate is the symmetric movement. The following equations can be derived by separating the symmetric and asymmetric functions in Eq. (18) as

$$2\cos\left(\frac{h}{2}\square_1\right)F^{(1)}+2\square_2^2T_2^{-2}\sum_{j=1}^{2}(-1)^{j-1}\cos\left(\frac{h}{2}\square_j\right)(W+F^{(1)})$$
$$-\cos\left(\frac{h}{2}\square_2\right)(W+F^{(1)})=0 \tag{18a}$$

$$\cos\left(\frac{h}{2}\square_2\right) f^{(1)} = 0 \tag{18b}$$

$$2\square_1 \sin\left(\frac{h}{2}\square_1\right) F^{(2)} + 2T_1^{-2}\sum_{j=1}^{2}(-1)^{j-1}\square_j \sin\left(\frac{h}{2}\square_j\right)\left(\square_1^2 F^{(2)} + E\right)$$
$$-\frac{1}{\kappa}\frac{\sin\left(\frac{h}{2}\square_2\right)}{\square_2}\left(\square_1^2 F^{(2)} + E\right) = 0 \tag{18c}$$

$$\square_2 \sin\left(\frac{h}{2}\square_2\right) f^{(2)} = 0 \tag{18d}$$

According to the entire function theory, the cosine and sine operators of Eqs. (18b) and (18d) can be expanded as follows,

$$\cos\left(\frac{h}{2}\square_2\right) f^{(1)} = \prod_{m=1}^{\infty}\left[1 - \frac{h^2\square_2^2}{(2m-1)^2\pi^2}\right] f^{(1)} \tag{19a}$$

$$\square_2 \sin\left(\frac{h}{2}\square_2\right) f^{(2)} = \square_2^2 \prod_{m=1}^{\infty}\left[1 - \frac{h^2\square_2^2}{4m^2\pi^2}\right] f^{(2)} \tag{19b}$$

The second-order wave equation of the following form can be obtained by truncating the infinite product series of Eq. (20) as

$$\nabla^2 f^{(2)} - T_2^2 f^{(2)} = 0 \tag{20}$$

Here, Eq. (20) represents the shear field of the stretching vibration.

Similarly, the following equation can be obtained by separating the asymmetric functions from the mid-plane of Eq. (17) as

$$-\frac{1}{2}\cos\left(\frac{h}{2}\square_1\right)\left[\frac{1}{\kappa}\left(\square_1^2 F^{(2)} + E\right) + T_2^2 F^{(2)}\right]$$
$$-\nabla^2\left[T_1^{-2}\sum_{j=1}^{2}(-1)^{j-1}\cos\left(\frac{h}{2}\square_j\right)\left(\square_1^2 F^{(2)} + E\right) + \cos\left(\frac{h}{2}\square_1\right) F^{(2)}\right] = \frac{1}{4\mu}q \tag{21}$$

According to Eqs. (20) and (21), the governing equation of the generalized displacement potential function E and $F^{(2)}$ of the stretching vibration of the plate can be obtained as

$$\begin{bmatrix} D_{11} & D_{12} \\ D_{21} & D_{22} \end{bmatrix}\begin{bmatrix} E \\ F^{(2)} \end{bmatrix} = \begin{bmatrix} 0 \\ \frac{q}{4\mu} \end{bmatrix} \tag{22}$$

where the expression of each operator is

$$D_{11} = 2T_1^{-2}\sum_{j=1}^{2}(-1)^{j-1}\frac{\sin\left(\frac{h}{2}\square_j\right)}{\square_j}\nabla^2 - 2\frac{\sin\left(\frac{h}{2}\square_1\right)}{\square_1} + \frac{1}{\kappa}\frac{\sin\left(\frac{h}{2}\square_2\right)}{\square_2}$$

$$D_{12} = 2T_1^{-2}\sum_{j=1}^{2}(-1)^{j-1}\frac{\sin\left(\frac{h}{2}\square_j\right)}{\square_j}\nabla^2\square_1^2 + \frac{1}{\kappa}\frac{\sin\left(\frac{h}{2}\square_2\right)}{\square_2}\square_1^2$$

$$D_{21} = T_1^{-2}\sum_{j=1}^{2}(-1)^{j-1}\cos\left(\frac{h}{2}\square_j\right)\nabla^2 - \frac{1}{2\kappa}\cos\left(\frac{h}{2}\square_1\right)$$

$$D_{22} = T_1^{-2}\sum_{j=1}^{2}(-1)^{j-1}\cos\left(\frac{h}{2}\square_j\right)\nabla^2\nabla^2 - \frac{1}{2\kappa}\cos\left(\frac{h}{2}\square_1\right)\nabla^2 + \cos\left(\frac{h}{2}\square_2\right)\nabla^2$$

According to the determinant of the operator matrix Eq. (22), the equation of the transverse normal strain function E can be obtained as

$$\begin{aligned}\Delta E = 2T_1^{-2}&\left[\frac{\sin\left(\frac{h}{2}\square_1\right)}{\square_1}\cos\left(\frac{h}{2}\square_2\right)-\frac{\sin\left(\frac{h}{2}\square_2\right)}{\square_2}\cos\left(\frac{h}{2}\square_1\right)\right]\nabla^2\nabla^2 E\\&-2\left[\frac{\sin\left(\frac{h}{2}\square_1\right)}{\square_1}\cos\left(\frac{h}{2}\square_2\right)-\frac{1}{\kappa}\frac{\sin\left(\frac{h}{2}\square_2\right)}{\square_2}\cos\left(\frac{h}{2}\square_1\right)\right]\nabla^2 E\\&-\frac{1}{2\kappa}\cos\left(\frac{h}{2}\square_1\right)\frac{\sin\left(\frac{h}{2}\square_2\right)}{\square_2}T_2^2 E=-\frac{1}{4\mu}D_{12}q\end{aligned}\tag{23}$$

After the truncation of the operator series of Eq. (23), the fourth-order wave equation of the stretching vibration of the plate can be obtained as

$$\nabla^2\nabla^2 E-12\left[\frac{1}{h^2}+\frac{2-\kappa^2}{24\left(1-\kappa\right)}T_2^2\right]\nabla^2 E+\frac{3}{1-\kappa}\left(\frac{1}{h^2}+\frac{1+3\kappa}{24}T_2^2\right)T_2^2 E=0\tag{24a}$$

$$\left[\left(3-2\kappa\right)\nabla^2-T_2^2-\frac{24}{h^2}\right]\left(\nabla^2-T_1^2\right)F=-\left[\left(3-4\kappa\right)\nabla^2-\left(1-2\kappa^2\right)T_2^2-\frac{24}{h^2}\left(1-2\kappa\right)\right]E\tag{24b}$$

$$\nabla^2 f-T_2^2 f=0\tag{24c}$$

where E, F, f are three generalized displacement functions of plate stretching vibration; $\nabla^2=\frac{\partial^2}{\partial x^2}+\frac{\partial^2}{\partial y^2}$ is Laplace operator; $T_j^2=\frac{1}{c_j^2}\frac{\partial^2}{\partial t^2}(j=1,2)$; c_1, c_2 are velocities of longitudinal wave and shear wave, respectively, $c_1^2=\frac{\lambda+2\mu}{\rho}, c_2^2=\frac{\mu}{\rho}$; $\kappa=\frac{1-2\nu}{2(1-\nu)}$; λ, μ are Lame constants; ν, ρ are Poisson's ratio and density, respectively, and h is plate thickness.

Without loss of generality, the solution of harmonic vibration is studied. Set

$$E=\tilde{E}\mathrm{e}^{-\mathrm{i}\omega t},\quad F=\tilde{F}\mathrm{e}^{-\mathrm{i}\omega t},\quad f=\tilde{f}\mathrm{e}^{-\mathrm{i}\omega t}\tag{25}$$

where ω is angular frequency of plate stretching, and i is the imaginary unit.

In the following analysis, the time factor and the symbol "$\sim$" in the generalized displacement functions are omitted. Substituting Eq. (25) into Eq. (24), the following equations can be obtained:

$$\Pi_{j=1}^2\left(\nabla^2+\alpha_j^2\right)E=0\tag{26a}$$

$$\nabla^2 f+k_2^2 f=0\tag{26b}$$

where $\alpha_j(j=1,2)$ are wave numbers which satisfy the algebraic equation

$$\alpha^4+12\left[\frac{1}{h^2}-\frac{2-\kappa^2}{24\left(1-\kappa\right)}k_2^2\right]\alpha^2-\frac{3}{1-\kappa}\left(\frac{1}{h^2}-\frac{1+3\kappa}{24}k_2^2\right)k_2^2=0, k_j^2=\omega^2/c_j^2\qquad(j=1,2)\tag{27}$$

Based on the refined theory of plate stretching, the expressions of generalized forces in plates are

$$N_x=\int_{-h/2}^{h/2}\sigma_x\mathrm{d}z,\quad N_{xy}=\int_{-h/2}^{h/2}\tau_{xy}\mathrm{d}z,\quad Q_x=\int_{-h/2}^{h/2}\tau_{zx}\mathrm{d}z=0\tag{28}$$

As the boundary condition of shear stress Q_x (zero-order moment) is automatically satisfied, the equation considering the one-order vanishing moment of the shear stress should be added as follows,

$$M_{Q_x}=\int_{-h/2}^{h/2}z\tau_{zx}\mathrm{d}z\tag{29}$$

Using complex functions and introducing complex variables $\zeta = x + \mathrm{i}y$ and $\overline{\zeta} = x - \mathrm{i}y$, Eqs. (28) and (29) can be converted to

$$N_x + N_y = (1-\nu) K \left\{ \frac{1-2\kappa}{\kappa} - \frac{1-\kappa}{\kappa} \left[1 + \frac{h^2}{24} \left(\alpha_m^2 - k_2^2 \right) \right] \alpha_m^2 \delta_m + \frac{h^2}{24} \left(\frac{2-3\kappa}{\kappa} \alpha_m^2 - \frac{1-2\kappa}{\kappa} k_2^2 \right) \right\} E \tag{30a}$$

$$N_y - N_x + 2\mathrm{i}N_{xy} = -4(1-\nu) K \frac{\partial^2}{\partial \zeta^2} \left\{ \left[\frac{h^2}{24} \frac{1-\kappa}{\kappa} + \delta_m - \frac{h^2}{24} \frac{1-2\kappa}{\kappa} \left(\alpha_m^2 - k_1^2 \right) \delta_m \right] E + \mathrm{i}f \right\} \tag{30b}$$

$$M_{Q_x} - \mathrm{i}M_{Q_y} = \frac{1}{2}(1-\nu) D \left[\frac{1}{\kappa} \left(\alpha_m^2 - k_1^2 \right) \delta_m - \frac{1-2\kappa}{\kappa} \right] \frac{\partial E}{\partial \zeta} \tag{30c}$$

in which B is stretching rigidity of the plate, and $B = \frac{Eh}{1-\nu^2}$.

Employing the conformal mapping method, the exterior region of noncircular cutout boundary in the ζ-plane can be mapped into a unit circle in the η-plane using the mapping function $\zeta = \Omega(\eta)$. The conformal mapping function can be taken as

$$\zeta = \Omega(\eta) = c\eta + \Phi(\eta) \tag{31}$$

where $\Phi(\eta)$ is a holomorphic function.

In polar coordinates (r, β), Eq. (30) can be written as follows,

$$\begin{aligned} N_r + N_\beta &= N_x + N_y \\ N_\beta - N_r + 2\mathrm{i}N_{r\beta} &= (N_y - N_x + 2\mathrm{i}N_{xy}) \exp(2\mathrm{i}\beta) \\ M_{Q_r} - \mathrm{i}M_{Q_\beta} &= \left(M_{Q_x} - \mathrm{i}M_{Q_y} \right) \exp(\mathrm{i}\beta) \end{aligned} \tag{32}$$

In the η-plane, Eq. (32) can be written as follows,

$$N_\rho + N_\theta = (1-\nu) B \left\{ \frac{1-2\kappa}{\kappa} - \frac{1-\kappa}{\kappa} \left[1 + \frac{h^2}{24} \left(\alpha_m^2 - k_2^2 \right) \right] \alpha_m^2 \delta_m + \frac{h^2}{24} \left(\frac{2-3\kappa}{\kappa} \alpha_m^2 - \frac{1-2\kappa}{\kappa} k_2^2 \right) \right\} E \tag{33a}$$

$$N_\theta - N_\rho + 2\mathrm{i}N_{\rho\theta} = -4(1-\nu) B \frac{\eta^2}{\rho} \frac{1}{\overline{\Omega'(\eta)}} \frac{\partial}{\partial \eta} \left(\frac{1}{\Omega'(\eta)} \frac{\partial}{\partial \eta} \right) \times \left\{ \left[\frac{h^2}{24} \frac{1-\kappa}{\kappa} + \delta_m - \frac{h^2}{24} \frac{1-2\kappa}{\kappa} \left(\alpha_m^2 - k_1^2 \right) \delta_m \right] E + \mathrm{i}f \right\} \tag{33b}$$

$$M_{Q_\rho} - \mathrm{i}M_{Q_\theta} = \frac{1}{2}(1-\nu) D \left[\frac{1}{\kappa} \left(\alpha_m^2 - k_1^2 \right) \delta_m - \frac{1-2\kappa}{\kappa} \right] \frac{\eta}{\rho \left| \Omega'(\eta) \right|} \frac{\partial}{\partial \eta} E \tag{33c}$$

The expressions of the generalized forces of the plate structure in the η-plane are

$$\begin{aligned} N_\rho = {} & \frac{(1-\nu)}{2} B \left\{ \frac{1-2\kappa}{\kappa} - \frac{1-\kappa}{\kappa} \left[1 + \frac{h^2}{24} \left(\alpha_m^2 - k_2^2 \right) \right] \alpha_m^2 \delta_m + \frac{h^2}{24} \left(\frac{2-3\kappa}{\kappa} \alpha_m^2 - \frac{1-2\kappa}{\kappa} k_2^2 \right) \right\} E \\ & + (1-\nu) K \left\{ \left[\frac{\eta^2}{\rho^2 \overline{\Omega'(\eta)}} \frac{\partial}{\partial \eta} \left(\frac{1}{\Omega'(\eta)} \frac{\partial}{\partial \eta} \right) + \frac{\bar{\eta}^2}{\rho^2 \Omega'(\eta)} \frac{\partial}{\partial \bar{\eta}} \left(\frac{1}{\overline{\Omega'(\eta)}} \frac{\partial}{\partial \bar{\eta}} \right) \right] \right. \\ & \times \left[\frac{h^2}{24} \frac{1-\kappa}{\kappa} + \delta_m - \frac{h^2}{24} \frac{1-2\kappa}{\kappa} \left(\alpha_m^2 - k_1^2 \right) \delta_m \right] E \\ & \left. + \left[\frac{\eta^2}{\rho^2 \overline{\Omega'(\eta)}} \frac{\partial}{\partial \eta} \left(\frac{1}{\Omega'(\eta)} \frac{\partial}{\partial \eta} \right) - \frac{\bar{\eta}^2}{\rho^2 \Omega'(\eta)} \frac{\partial}{\partial \bar{\eta}} \left(\frac{1}{\overline{\Omega'(\eta)}} \frac{\partial}{\partial \bar{\eta}} \right) \right] \mathrm{i}f \right\} \end{aligned} \tag{34a}$$

$$N_\theta = \frac{1-\nu}{2}B\left\{\frac{1-2\kappa}{\kappa}-\frac{1-\kappa}{\kappa}\left[1+\frac{h^2}{24}\left(\alpha_m^2-k_2^2\right)\right]\alpha_m^2\delta_m+\frac{h^2}{24}\left(\frac{2-3\kappa}{\kappa}\alpha_m^2-\frac{1-2\kappa}{\kappa}k_2^2\right)\right\}E$$
$$-(1-\nu)K\left\{\left[\frac{\eta^2}{\rho^2\overline{\Omega'(\eta)}}\frac{\partial}{\partial\eta}\left(\frac{1}{\Omega'(\eta)}\frac{\partial}{\partial\eta}\right)+\frac{\bar{\eta}^2}{\rho^2\Omega'(\eta)}\frac{\partial}{\partial\bar{\eta}}\left(\frac{1}{\overline{\Omega'(\eta)}}\frac{\partial}{\partial\bar{\eta}}\right)\right]\right.$$
$$\times\left[\frac{h^2}{24}\left(\frac{1}{\kappa}-1\right)+\delta_m-\frac{h^2}{24}\frac{1-2\kappa}{\kappa}\left(\alpha_m^2-k_1^2\right)\delta_m\right]E$$
$$\left.+\left[\frac{\eta^2}{\rho^2\overline{\Omega'(\eta)}}\frac{\partial}{\partial\eta}\left(\frac{1}{\Omega'(\eta)}\frac{\partial}{\partial\eta}\right)-\frac{\bar{\eta}^2}{\rho^2\Omega'(\eta)}\frac{\partial}{\partial\bar{\eta}}\left(\frac{1}{\overline{\Omega'(\eta)}}\frac{\partial}{\partial\bar{\eta}}\right)\right]\mathrm{i}f\right\} \tag{34b}$$

$$N_{\rho\theta} = (1-\nu)B\mathrm{i}\left\{\left[\frac{\eta^2}{\rho^2\overline{\Omega'(\eta)}}\frac{\partial}{\partial\eta}\left(\frac{1}{\Omega'(\eta)}\frac{\partial}{\partial\eta}\right)-\frac{\bar{\eta}^2}{\rho^2\Omega'(\eta)}\frac{\partial}{\partial\bar{\eta}}\left(\frac{1}{\overline{\Omega'(\eta)}}\frac{\partial}{\partial\bar{\eta}}\right)\right]\right.$$
$$\times\left[\frac{h^2}{24}\left(\frac{1}{\kappa}-1\right)+\delta_m-\frac{h^2}{24}\frac{1-2\kappa}{\kappa}\left(\alpha_m^2-k_1^2\right)\delta_m\right]E$$
$$\left.+\mathrm{i}\left[\frac{\eta^2}{\rho^2\overline{\Omega'(\eta)}}\frac{\partial}{\partial\eta}\left(\frac{1}{\Omega'(\eta)}\frac{\partial}{\partial\eta}\right)+\frac{\bar{\eta}^2}{\rho^2\Omega'(\eta)}\frac{\partial}{\partial\bar{\eta}}\left(\frac{1}{\overline{\Omega'(\eta)}}\frac{\partial}{\partial\bar{\eta}}\right)\right]f\right\} \tag{34c}$$

$$M_{Q_\rho} = (1-\nu)B\frac{h^2}{48}\left[\frac{1}{\kappa}\left(\alpha_m^2-k_1^2\right)\delta_m-\frac{1-2\kappa}{\kappa}\right]\left[\frac{\eta}{\rho}\frac{1}{|\Omega'(\eta)|}\frac{\partial}{\partial\eta}+\frac{\bar{\eta}}{\rho}\frac{1}{|\Omega'(\eta)|}\frac{\partial}{\partial\bar{\eta}}\right]E \tag{34d}$$

$$M_{Q_\theta} = (1-\nu)B\frac{h^2}{48}\left[\frac{1}{\kappa}\left(\alpha_m^2-k_1^2\right)\delta_m-\frac{1-2\kappa}{\kappa}\right]\left[\frac{\eta}{\rho}\frac{1}{|\Omega'(\eta)|}\frac{\partial}{\partial\eta}-\frac{\bar{\eta}}{\rho}\frac{1}{|\Omega'(\eta)|}\frac{\partial}{\partial\bar{\eta}}\right]\mathrm{i}E \tag{34e}$$

The general solution of the scattering wave described by the vibration Eq. (24) of the stretching plate can be written as follows,

$$E=\sum_{m=1}^{2}\sum_{n=-\infty}^{\infty}A_{mn}\mathrm{H}_n^{(1)}\left(\alpha_m|\Omega(\eta)|\right)\left\{\frac{\Omega(\eta)}{|\Omega(\eta)|}\right\}^n \tag{35a}$$

$$F=\sum_{m=1}^{2}\sum_{n=-\infty}^{\infty}A_{mn}\delta_m\mathrm{H}_n^{(1)}\left(\alpha_m|\Omega(\eta)|\right)\left\{\frac{\Omega(\eta)}{|\Omega(\eta)|}\right\}^n \tag{35b}$$

$$f=\sum_{n=-\infty}^{\infty}B_n\mathrm{K}_n\left(k_2|\Omega(\eta)|\right)\left\{\frac{\Omega(\eta)}{|\Omega(\eta)|}\right\}^n \tag{35c}$$

where $\delta_j(j=1,2)$ is the proportional coefficient of the scattering wave function, and $\delta_j=\frac{(3-4\kappa)\alpha_j^2h^2-\left(1-2\kappa^2\right)k_2^2h^2+24(1-2\kappa)}{\left[(3-2\kappa)\alpha_j^2h^2-k_2^2h^2+24\right]\left(\alpha_j^2-k_1^2\right)}$; $\mathrm{H}_n^{(1)}(\cdot)$ denotes Hankel function; $\mathrm{K}_n(\cdot)$ denotes Bessel function of imaginary argument; and $A_{mn}(m=1,2)$ and B_n are mode coefficients of the scattered wave, which can be determined by the cutout boundary conditions.

3. Excitation of Incident Waves and Total Wave Fields

As a plate with two cutouts is investigated in Fig. 1, we consider a tension–compression wave propagating along the positive direction of x-axis. Based on the constructive interference theory of wave fields, the incident wave can be proposed as

$$E^{(i)}=E_0\mathrm{e}^{\mathrm{i}\alpha_1x}=E_0\sum_{n=-\infty}^{\infty}(\mathrm{i})^n\mathrm{J}_n(\alpha_1r)\mathrm{e}^{\mathrm{i}n\beta} \tag{36a}$$

$$F^{(i)}=\delta_1E^{(i)} \tag{36b}$$

$$f^{(i)}=0 \tag{36c}$$

The total wave field of the elastic wave of plates can be expressed as

$$E = E^{(i)} + \sum_{j=1}^{2} E^{(s)} = E_0 \mathrm{e}^{\mathrm{i}\alpha_1 x} + \sum_{j=1}^{2} \sum_{n=-\infty}^{\infty} \sum_{m=1}^{2} A_{nm}^{j} \mathrm{H}_n^{(1)}(\alpha_m |\Omega(\eta_j)|) \left\{ \frac{\Omega(\eta_j)}{|\Omega(\eta_j)|} \right\}^n \tag{37a}$$

$$F = F^{(i)} + \sum_{j=1}^{2} F^{(s)} = \delta_1 E_0 \mathrm{e}^{\mathrm{i}\alpha_1 x} + \sum_{j=1}^{2} \sum_{n=-\infty}^{\infty} \sum_{m=1}^{2} A_{nm}^{j} \delta_m \mathrm{H}_n^{(1)}(\alpha_m |\Omega(\eta_j)|) \left\{ \frac{\Omega(\eta_j)}{|\Omega(\eta_j)|} \right\}^n \tag{37b}$$

$$f = f^{(i)} + \sum_{j=1}^{2} f^{(s)} = \sum_{j=1}^{2} \sum_{n=-\infty}^{\infty} B_n^j \mathrm{K}_n(\alpha_3 |\Omega(\eta_j)|) \left\{ \frac{\Omega(\eta_j)}{|\Omega(\eta_j)|} \right\}^n \tag{37c}$$

4. Determination of Mode Coefficients Satisfying Boundary Conditions

The case of free boundary condition is investigated. In the η-plane, it meets six boundary conditions as follows,

$$N_\rho^j\big|_{\rho=a} = 0, N_{\rho\theta}^j\big|_{\rho=a} = 0, M_{Q_\rho}^j\big|_{\rho=a} = 0 \ (j = 1, 2) \tag{38}$$

Substituting Eqs. (34a), (34c), (34d) and (37) into Eq. (38), the infinite linear algebraic equations to determine the six mode coefficients $A_{n1}^j, A_{n2}^j, B_n^j$ can be given as

$$\sum_{j=1}^{6} \sum_{n=-\infty}^{\infty} K_n^{ij} X_n^j = K_i \qquad (i = 1, 2, 3, 4, 5, 6) \tag{39}$$

Multiplying Eq. (39) by $\mathrm{e}^{-\mathrm{i}s\theta}$, and integrating between $-\pi$ and π, we can get the expression

$$\sum_{n=-\infty}^{\infty} \boldsymbol{K}_{ns} \boldsymbol{X}_n = \boldsymbol{K}_s \tag{40}$$

where $\boldsymbol{K}_{ns} = \frac{1}{2\pi} \int_{-\pi}^{\pi} \boldsymbol{K}_n \exp(-\mathrm{i}s\theta_j) \mathrm{d}\theta_j, \boldsymbol{K}_s = \frac{1}{2\pi} \int_{-\pi}^{\pi} \boldsymbol{K} \exp(-\mathrm{i}s\theta_j) \mathrm{d}\theta_j$

$$\boldsymbol{K}_n = \begin{bmatrix} K_{11}^n & K_{12}^n & K_{13}^n & K_{14}^n & K_{15}^n & K_{16}^n \\ K_{21}^n & K_{22}^n & K_{23}^n & K_{24}^n & K_{25}^n & K_{26}^n \\ K_{31}^n & K_{32}^n & 0 & K_{34}^n & K_{35}^n & K_{36}^n \\ K_{41}^n & K_{42}^n & K_{43}^n & K_{44}^n & K_{45}^n & K_{46}^n \\ K_{51}^n & K_{52}^n & K_{53}^n & K_{54}^n & K_{55}^n & K_{56}^n \\ K_{61}^n & K_{62}^n & K_{63}^n & K_{64}^n & K_{65}^n & 0 \end{bmatrix}, \quad \boldsymbol{X}_n = \begin{bmatrix} A_{n1}^1 \\ A_{n2}^1 \\ B_n^1 \\ A_{n1}^2 \\ A_{n2}^2 \\ B_n^2 \end{bmatrix}, \quad \boldsymbol{K}_s = \begin{bmatrix} K_1 \\ K_2 \\ K_3 \\ K_4 \\ K_5 \\ K_6 \end{bmatrix}$$

The elements of $\boldsymbol{K}_n$ and $\boldsymbol{K}_s$ see "Appendix".

The dynamic stress concentration factor (DSCF) is defined as the ratio of stress due to the total wave at a point to the stress due to the incident wave (without the scatterer) at the same point [3]. In term of the definition, for the plate with two cutouts, the DSCFs around the m-th cutout can be expressed by

$$\sigma_\theta^* = \sigma_\theta / \sigma_0 = \left(\sigma_\theta^{(i)} + \sigma_\theta^{(s)} \right) / \sigma_0 \tag{41}$$

where

$$\sigma_\theta^{(i)} = \mu_{\mathrm{M}} \left\{ \left[\frac{1-2\kappa}{\kappa} - \frac{1-\kappa}{\kappa} \alpha_1^2 \delta_1 \right] + \alpha_1^2 \delta_1 \mathrm{Re} \left(\frac{\eta}{\bar{\eta}} \frac{\Omega'(\eta)}{\overline{\Omega'(\eta)}} \right) \right\} \exp \left[\frac{\mathrm{i}\alpha_1}{2} \mathrm{Re}(\Omega'(\eta)) \right]$$

$$\sigma_\theta^{(s)} = \mu_{\mathrm{M}} \sum_{j=1}^{2} \sum_{m=1}^{2} \sum_{n=-\infty}^{\infty} \left(\frac{1-2\kappa}{\kappa} - \frac{1-\kappa}{\kappa} \alpha_m^2 \delta_m \right) A_{mn} \mathrm{H}_n^{(1)}(\alpha_m r_j) \mathrm{e}^{\mathrm{i}n\theta_j}$$

$$- 2\mu_{\mathrm{M}} \left\{ \sum_{j=1}^{2} \sum_{m=1}^{2} \sum_{n=-\infty}^{\infty} A_{mn} \frac{\alpha_m^2 \delta_m}{4} \left[\frac{\eta_i^2}{\rho_i^2} \frac{\Omega'(\eta_i)}{\overline{\Omega'(\eta_i)}} \mathrm{H}_{n-2}^{(1)}(\alpha_m r_j) \mathrm{e}^{\mathrm{i}(n-2)\theta_j} \right. \right.$$

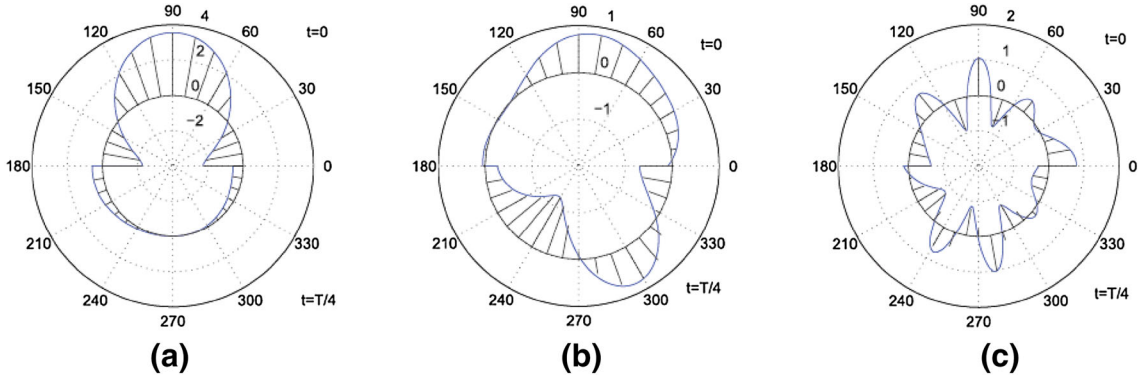

Fig. 2. Dynamic stress in stretching plates around cutouts, where α_1 denotes dimensionless incident wave number and L/a denotes cutout-spacing. **a** $\alpha_1 a = 0.1, L/a = 2.1$, **b** $\alpha_1 a = 1.0, L/a = 2.1$, **c** $\alpha_1 a = 5.0, L/a = 2.1$

$$+ \frac{\bar{\eta}_i^2}{\rho_i^2}\frac{\overline{\Omega'(\eta_i)}}{\Omega'(\eta_i)}\mathrm{H}_{n+2}^{(1)}(\alpha_m r_j)\mathrm{e}^{\mathrm{i}(n+2)\theta_j}\Bigg] + \frac{k_2^2}{4}\mathrm{i}\sum_{j=1}^{2}\sum_{n=-\infty}^{\infty} B_n$$
$$\times \left[\frac{\eta_i^2}{\rho_i^2}\frac{\Omega'(\eta_i)}{\overline{\Omega'(\eta_i)}}\mathrm{K}_{n-2}(k_2 r_j)\mathrm{e}^{\mathrm{i}(n-2)\theta_j} - \frac{\bar{\eta}_i^2}{\rho_i^2}\frac{\overline{\Omega'(\eta_i)}}{\Omega'(\eta_i)}\mathrm{K}_{n+2}(k_2 r_j)\mathrm{e}^{\mathrm{i}(n+2)\theta_j}\right]\Bigg\}$$

σ_0 is the amplitude of the normal stress of the incident wave along the x-axis direction, and $\sigma_0 = \left[\lambda_{\mathrm{M}}\left(1-\delta_1\alpha_1^2\right) - 2\mu_{\mathrm{M}}\delta_1\alpha_1^2\right]E_0$.

5. Numerical Examples and Discussion

Fatigue failures often occur in the regions with high stress concentration, so an understanding of the distribution of the dynamic stress around the inclusion is quite useful in structural design. According to the expression of DSCF induced by tension–compression wave, the DSCFs around the cutouts are simulated by using MATLAB. We put forward the program to calculate the dynamic stress concentration factor in the plate with two cutouts. For the convenience of calculation, in the following analysis, the dimensionless variables are employed. To accomplish this step, a representative length scale a, which is the radius of the cutout, is introduced. The following dimensionless variables and quantities are chosen for numerical calculation: the incident wavenumber $\alpha_1 a = 0.01{-}5.0$, the thickness of plate $h/a = 0.2{-}10.0$, the cutout-spacing $L/a = 2.1{-}12.0$, Poisson's ratio $\nu = 0.3$, and $n = 10$.

The numerical results of DSCFs for different plates with two cutouts by using the refined dynamic equation are depicted in Figs. 2 and 3, which illustrate the angular distributions of the dynamic stress around the cutouts with different wave numbers, cutout-spacings, and plate thicknesses. For each figure, the upper half illustrates the dynamic stress distributions when $t = 0$, while the lower half illustrates the dynamic stress distributions when $t = T/4$. Figures 4 and 5 show the dynamic stress concentration factors versus the dimensionless wave number $\alpha_1 a$.

Figure 2a–c displays the angular distribution of the DSCFs around the circular cutouts in thick plates ($h/a = 10.0$) when the cutout-spacing is small ($L/a = 2.1$). Because of the mutual influence between two cutouts, when the incident wave number is $\alpha_1 a = 0.1$, at time $t = 0$, the maximum DSCF (the value is 3.91 in Fig. 2) is 19% greater than that of the plane stress problem in Ref. [3] (the value is 3.28). The DSCF values are close to zero at time $t = T/4$, which agrees with plane stress problem. When the incident wave number is $\alpha_1 a = 1.0$, at time $t = 0$, the maximum DSCF is less than one, differing from that of the plane stress problem in Ref. [3]. The maximum DSCF values at time $t = T/4$ are close to zero at time $t = 0$. It is noted that the maximum DSCF values at time $t = T/4$ are near the position of $\theta = 5\pi/3$. When the incident wave number is $\alpha_1 a = 5.0$, at time $t = 0$, the maximum DSCF is close to 1.0. It is noteworthy that the DSCFs fluctuate. The large values are near the positions of $\theta = 0, \theta = 5\pi/18, \theta = 13\pi/18$, and the negative values are close to -1.0 near the

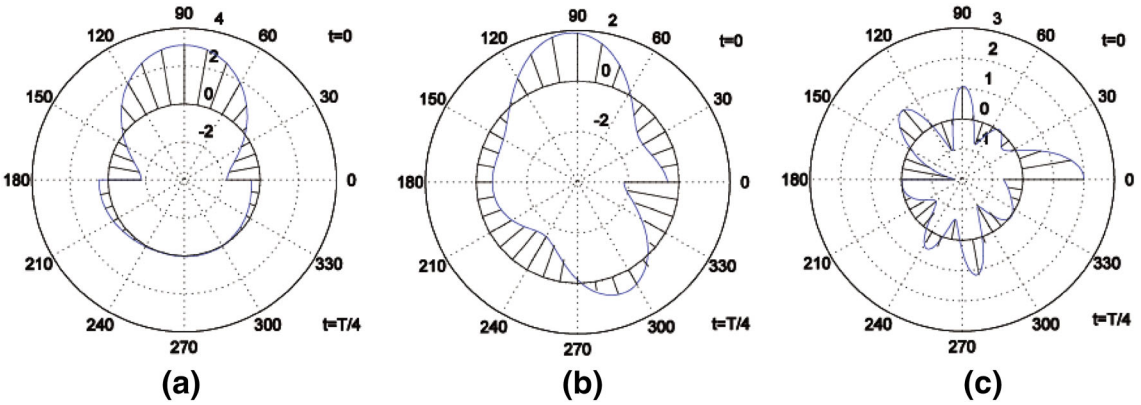

Fig. 3. Dynamic stress in stretching plates around cutouts with different cutout-spacing, where α_1 denotes dimensionless incident wave number and L/a denotes cutout-spacing. **a** $\alpha_1 a = 0.1, L/a = 6.0$, **b** $\alpha_1 a = 1.0, L/a = 8.0$, **c** $\alpha_1 a = 5.0, L/a = 11.0$

positions of $\theta = 4\pi/9, \theta = 11\pi/18$. The maximum DSCF values at time $t = T/4$ are close to -1.0 near the position of $\theta = 4\pi/3, 14\pi/9$.

Figure 3a–c displays the angular distribution of the DSCFs around the circular cutouts in thick plates ($h/a = 10.0$) when the cutout-spacing is large. The larger is the cutout-spacing, the smaller is the mutual influence between two cutouts. When the incident wave number is $\alpha_1 a = 0.1$ and the cutout-spacing is $L/a = 6.0$, the angular distribution of the DSCFs is almost equal to that of the DSCFs with one single cutout in Ref. [15], which means that the minimum cutout-spacing to ensure zero mutual influence between cutouts is $L/a = 6.0$. When the incident wave number is $\alpha_1 a = 1.0$ and the cutout-spacing is $L/a = 8.0$, the angular distribution of the DSCFs is almost equal to that of the DSCFs with one single cutout in Ref. [15]. When the incident wave number is $\alpha_1 a = 5.0$, the minimum cutout-spacing to ensure zero mutual influence between cutouts is about $L/a = 11.0$. Thus, it can be seen that the larger is the incident wave number, the wider is the range of mutual influence between cutouts.

As shown in Figs. 4 and 5, the DSCF in the low-frequency region is higher than that in the high-frequency area, and the DSCF in the high-frequency area is kept near 1.0. When $a/h = 0.1$, the DSCF varies in the low-frequency region, quickly reaches the minimum, and then gradually tends to be stable. When $a/h = 0.5$, there is stagnation before reaching the minimum. When $a/h = 1.0, a/h = 2.0, a/h = 5.0$ is applied, the DSCF decreases gradually and becomes stable near 3.0, and the minimum DSCF increases. It can be seen that with the decrease in the thickness of the plate, the stress varies slowly in the low-frequency region.

6. Conclusions

In this paper, based on the refined dynamic equation of stretching thick plates, and using the complex variable method and conformal mapping method, the elastic tension–compression wave scattering and dynamic stress concentration in plates with two cutouts are investigated. According to the analysis of the above numerical results, we can conclude that the parameters such as incident wave number, thickness of plate, and cutout-spacing have great effects on dynamic stress distributions. It is shown that:

At a low frequency and a small thickness of the plate, the numerical results obtained using the refined theory approach those obtained using the plane stress theory (see Ref. [3]). At a high frequency and a great thickness of the plate, the numerical results obtained using the refined theory are far from those obtained using the plane stress theory. Especially, as the thickness is great ($a/h = 0.1$), using the refined equation, the DSCF may approach the maximum value of 3.91, which is over 19% greater than that of the plane stress problem (the maximum value is 3.28). Such a big error is not allowed in engineering, which needs great attention. It shows good agreement with the conclusion verified by many dynamicists that the solution of the plane stress problem only applies to large wavelength

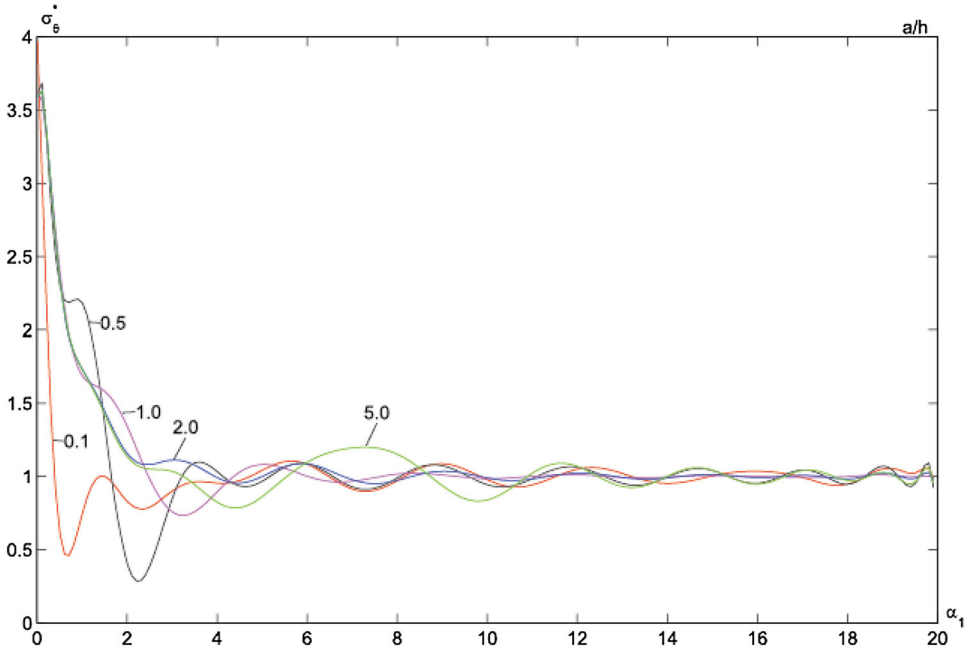

Fig. 4. Dynamic stress between two nearby cutouts in stretching plates versus dimensionless wave numbers ($\nu = 0.3, \theta = \pi/2, L/a = 2.1$)

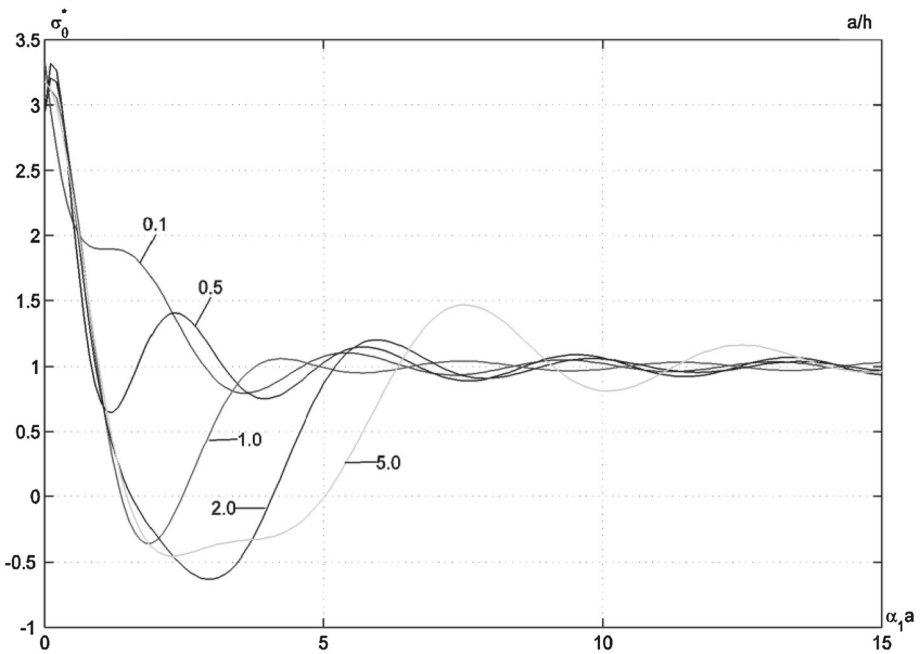

Fig. 5. Dynamic stress between two away cutouts in stretching plates versus dimensionless wave numbers ($\nu = 0.3, \theta = \pi/2, L/a = 12.0$)

and low-frequency incident wave. Hence, it is of the importance to derive the refined plate theory for elastodynamics of thick plates. Besides, as the incident waves are at low frequency, the minimum cutout-spacing to ensure zero mutual influence between cutouts is small; as the incident waves are at high frequency, the minimum cutout-spacing to ensure zero mutual effect between cutouts is great. Therefore, the cutout-spacings should be distributed rationally in the structural design.

In this paper, the refined equation is derived without using any engineering hypotheses. Therefore, the results in this paper are more accurate, which can be applied to the condition of thick-walled structures and high-frequency vibration. Furthermore, it is worth mentioning that the numerical simulation on two circular cutouts is a typical example, and if proper mapping functions $\Omega(\zeta)$ are given, the application of this method to solving the problem on scattering of elastic waves can be spread to arbitrary-shaped cutouts, providing a unified and standardized method for analyzing dynamic stress concentrations around cutouts. The theory and the numerical results in this paper can be used for the dynamic analysis and strength design of engineering thick-walled structures, high-precision structural design and lightweight structural design.

Acknowledgements. This work is supported by the Natural Science Foundation of Zhejiang Province of China (Grant No. LQ17E050011), the National Natural Science Foundation of China (Grant No. 51775154), the Natural Science Foundation of Zhejiang Province of China (Grant No. LQ17E090007) and the Key Project of Natural Science Foundation of Zhejiang Province of China (Grant No. LQ17E050011).

References

[1] Savin GN. Stress concentration around holes. Oxford: Pergamon Press; 1961.
[2] Muskhelishvili NI. Some basic problems of the mathematical theory of elasticity. Berlin: Springer; 2013.
[3] Pao YH, Maw CC. Diffraction of elastic wave and dynamic stress concentration. New York: Crane Russak and Company; 1973.
[4] Liu DK, Hu C. Scattering of flexural wave and dynamic stress concentration in mindlin thick plates with a cutout. Acta Mech Sin. 1996;12(2):169–85.
[5] Liu DK, Gai BZ, Tao GY. Applications of the method of complex functions to dynamic stress concentrations. Wave Motion. 1982;4(3):293–304.
[6] Shimpi RP, Patel HG. A two variable refined plate theory for orthotropic plate analysis. Int J Solids Struct. 2006;43(22–23):6783–99.
[7] Pao YH. Elastic waves in solids. J Appl Mech. 1983;50(4):1152–64.
[8] Bedford A, Drumheller DS. Introduction to elastic wave propagation. London: Wiley; 1994.
[9] Saada AS. Elasticity: theory and applications. Amsterdam: Elsevier; 2013.
[10] Eringen AC, Suhubi ES. Elastodynamics, volume II linear theory. New York: Academic Press; 1975.
[11] Sreelakshmi T, Rama E, Somaiah K. Effect of rotation on longitudinal wave propagation in an elastic solid with a cylindrical hole. Proc Eng. 2015;127:660–4.
[12] Khurana A, Tomar SK. Wave propagation in nonlocal microstretch solid. Appl Math Model. 2016;40(11–12):5858–75.
[13] Somaiah K. Propagation of plane waves in micro-stretch elastic solid in special case. Glob J Pure Appl Math. 2017;13(6):2143–51.
[14] Hu C, Cao TG, Zhou CP. Dynamic stress concentrations in infinite plates with a circular cutout based on refined theory. Arch Appl Mech. 2016;87(2):1–17.
[15] Hu C, Zhou CP, Ni B, Liu DK. Dynamic stress concentrations in thick plates with an arbitrary cutout by using the refined theory. Chin J Solid Mech. 2013;34(4):410–6 **(in Chinese)**.
[16] Zhou CP, Hu C, Ma F, Liu DK. Dynamic stress concentrations in thick plates with two holes based on refined theory. Appl Math Mech (English Edn). 2014;35(12):1591–606.

Appendix

The elements of matrices $\boldsymbol{K}_n$ and $\boldsymbol{K}_s$ are as follows.

$$K_{1m}^{n} = \left\{ \frac{1-2\kappa}{\kappa} - \frac{1-\kappa}{\kappa}\left[1+\frac{h^2}{24}\left(\alpha_m^2-k_2^2\right)\right]\alpha_m^2\delta_m + \frac{h^2}{24}\left(\frac{2-3\kappa}{\kappa}\alpha_m^2 - \frac{1-2\kappa}{\kappa}k_2^2\right)\right\} \mathrm{H}_n^{(1)}\left(\alpha_m r_1\right)\mathrm{e}^{\mathrm{i}n\theta_1} + \frac{\alpha_m^2}{2}\left[\frac{h^2}{24}\left(\frac{1}{\kappa}-1\right) + \delta_m - \frac{h^2}{24}\frac{1-2\kappa}{\kappa}\left(\alpha_m^2-k_1^2\right)\delta_m\right]$$

$$\times\left[\frac{\eta_1^2}{\rho_1^2}\frac{\Omega'(\eta_1)}{\overline{\Omega'(\eta_1)}}\mathrm{H}_{n-2}^{(1)}(\alpha_m r_1)\mathrm{e}^{\mathrm{i}(n-2)\theta_1}+\frac{\bar{\eta}_1^2}{\rho_1^2}\frac{\overline{\Omega'(\eta_1)}}{\Omega'(\eta_1)}\mathrm{H}_{n+2}^{(1)}(\alpha_m r_1)\mathrm{e}^{\mathrm{i}(n+2)\theta_1}\right]\quad(m=1,2)$$

$$K_{13}^n=\frac{k_2^2}{2}\mathrm{i}\left[\frac{\eta_1^2}{\rho_1^2}\frac{\Omega'(\eta_1)}{\overline{\Omega'(\eta_1)}}\mathrm{K}_{n-2}(k_2 r_1)\mathrm{e}^{\mathrm{i}(n-2)\theta_1}-\frac{\bar{\eta}_1^2}{\rho_1^2}\frac{\overline{\Omega'(\eta_1)}}{\Omega'(\eta_1)}\mathrm{K}_{n+2}(k_2 r_1)\mathrm{e}^{\mathrm{i}(n+2)\theta_1}\right]$$

$$K_{1m}^n=\left\{\frac{1-2\kappa}{\kappa}-\frac{1-\kappa}{\kappa}\left[1+\frac{h^2}{24}\left(\alpha_{m-3}^2-k_2^2\right)\right]\alpha_{m-3}^2\delta_{m-3}\right.$$
$$\left.+\frac{h^2}{24}\left(\frac{2-3\kappa}{\kappa}\alpha_{m-3}^2-\frac{1-2\kappa}{\kappa}k_2^2\right)\right\}\mathrm{H}_n^{(1)}\left(\alpha_{m-3}r_2\right)\mathrm{e}^{\mathrm{i}n\theta_2}$$
$$+\frac{\alpha_{m-3}^2}{2}\left[\frac{h^2}{24}\left(\frac{1}{\kappa}-1\right)+\delta_{m-3}-\frac{h^2}{24}\frac{1-2\kappa}{\kappa}\left(\alpha_{m-3}^2-k_1^2\right)\delta_{m-3}\right]$$
$$\times\left[\frac{\eta_1^2}{\rho_1^2}\frac{\Omega'(\eta_1)}{\overline{\Omega'(\eta_1)}}\mathrm{H}_{n-2}^{(1)}(\alpha_{m-3}r_2)\mathrm{e}^{\mathrm{i}(n-2)\theta_2}+\frac{\bar{\eta}_1^2}{\rho_1^2}\frac{\overline{\Omega'(\eta_1)}}{\Omega'(\eta_1)}\mathrm{H}_{n+2}^{(1)}(\alpha_{m-3}r_2)\mathrm{e}^{\mathrm{i}(n+2)\theta_2}\right]\quad(m=4,5)$$

$$K_{16}^n=\frac{k_2^2}{2}\mathrm{i}\left[\frac{\eta_1^2}{\rho_1^2}\frac{\Omega'(\eta_1)}{\overline{\Omega'(\eta_1)}}\mathrm{K}_{n-2}(k_2 r_2)\mathrm{e}^{\mathrm{i}(n-2)\theta_2}-\frac{\bar{\eta}_1^2}{\rho_1^2}\frac{\overline{\Omega'(\eta_1)}}{\Omega'(\eta_1)}\mathrm{K}_{n+2}(k_2 r_2)\mathrm{e}^{\mathrm{i}(n+2)\theta_2}\right]$$

$$K_{2m}^n=\frac{\alpha_m^2}{2}\left[\frac{\eta_1^2}{\rho_1^2}\frac{\Omega'(\eta_1)}{\overline{\Omega'(\eta_1)}}\mathrm{H}_{n-2}^{(1)}(\alpha_m r_1)\mathrm{e}^{\mathrm{i}(n-2)\theta_1}-\frac{\bar{\eta}_1^2}{\rho_1^2}\frac{\overline{\Omega'(\eta_1)}}{\Omega'(\eta_1)}\mathrm{H}_{n+2}^{(1)}(\alpha_m r_1)\mathrm{e}^{\mathrm{i}(n+2)\theta_1}\right]$$
$$\times\left[\frac{h^2}{24}\left(\frac{1}{\kappa}-1\right)+\delta_m-\frac{h^2}{24}\frac{1-2\kappa}{\kappa}\left(\alpha_m^2-k_1^2\right)\delta_m\right]\qquad(m=1,2)$$

$$K_{23}^n=\frac{k_2^2}{2}\mathrm{i}\left[\frac{\eta_1^2}{\rho_1^2}\frac{\Omega'(\eta_1)}{\overline{\Omega'(\eta_1)}}\mathrm{K}_{n-2}(k_2 r_1)\mathrm{e}^{\mathrm{i}(n-2)\theta_1}+\frac{\bar{\eta}_1^2}{\rho_1^2}\frac{\overline{\Omega'(\eta_1)}}{\Omega'(\eta_1)}\mathrm{K}_{n+2}(k_2 r_1)\mathrm{e}^{\mathrm{i}(n+2)\theta_1}\right]$$

$$K_{2m}^n=\frac{\alpha_{m-3}^2}{2}\left[\frac{\eta_1^2}{\rho_1^2}\frac{\Omega'(\eta_1)}{\overline{\Omega'(\eta_1)}}\mathrm{H}_{n-2}^{(1)}(\alpha_{m-3}r_2)\mathrm{e}^{\mathrm{i}(n-2)\theta_2}-\frac{\bar{\eta}_1^2}{\rho_1^2}\frac{\overline{\Omega'(\eta_1)}}{\Omega'(\eta_1)}\mathrm{H}_{n+2}^{(1)}(\alpha_{m-3}r_2)\mathrm{e}^{\mathrm{i}(n+2)\theta_2}\right]$$
$$\times\left[\frac{h^2}{24}\left(\frac{1}{\kappa}-1\right)+\delta_{m-3}-\frac{h^2}{24}\frac{1-2\kappa}{\kappa}\left(\alpha_{m-3}^2-k_1^2\right)\delta_{m-3}\right]\quad(m=4,5)$$

$$K_{26}^n=\frac{k_2^2}{2}\mathrm{i}\left[\frac{\eta_1^2}{\rho_1^2}\frac{\Omega'(\eta_1)}{\overline{\Omega'(\eta_1)}}\mathrm{K}_{n-2}(k_2 r_2)\mathrm{e}^{\mathrm{i}(n-2)\theta_2}+\frac{\bar{\eta}_1^2}{\rho_1^2}\frac{\overline{\Omega'(\eta_1)}}{\Omega'(\eta_1)}\mathrm{K}_{n+2}(k_2 r_2)\mathrm{e}^{\mathrm{i}(n+2)\theta_2}\right]$$

$$K_{3m}^n=\alpha_m\left[\frac{1}{\kappa}\left(\alpha_m^2-k_1^2\right)\delta_m-\frac{1-2\kappa}{\kappa}\right]\left[\frac{\eta_1}{\rho_1}\frac{\Omega'(\eta_1)}{|\Omega'(\eta_1)|}\mathrm{H}_{n-1}^{(1)}(\alpha_m r_1)\mathrm{e}^{\mathrm{i}(n-1)\theta_1}\right.$$
$$\left.-\frac{\bar{\eta}_1}{\rho_1}\frac{\overline{\Omega'(\eta_1)}}{|\Omega'(\eta_1)|}\mathrm{H}_{n+1}^{(1)}(\alpha_m r_1)\mathrm{e}^{\mathrm{i}(n+1)\theta_1}\right]\quad m=1,2)$$

$$K_{3m}^n=\alpha_{m-3}\left[\frac{1}{\kappa}\left(\alpha_{m-3}^2-k_1^2\right)\delta_{m-3}-\frac{1-2\kappa}{\kappa}\right]\left[\frac{\eta_1}{\rho_1}\frac{\Omega'(\eta_1)}{|\Omega'(\eta_1)|}\mathrm{H}_{n-1}^{(1)}(\alpha_{m-3}r_2)\mathrm{e}^{\mathrm{i}(n-1)\theta_2}\right.$$
$$\left.-\frac{\bar{\eta}_1}{\rho_1}\frac{\overline{\Omega'(\eta_1)}}{|\Omega'(\eta_1)|}\mathrm{H}_{n+1}^{(1)}(\alpha_{m-3}r_2)\mathrm{e}^{\mathrm{i}(n+1)\theta_2}\right]\quad(m=4,5)$$

$$K_{4m}^n=\left\{\frac{1-2\kappa}{\kappa}-\frac{1-\kappa}{\kappa}\left[1+\frac{h^2}{24}\left(\alpha_m^2-k_2^2\right)\right]\alpha_m^2\delta_m+\frac{h^2}{24}\left(\frac{2-3\kappa}{\kappa}\alpha_m^2-\frac{1-2\kappa}{\kappa}k_2^2\right)\right\}$$
$$\times\mathrm{H}_n^{(1)}\left(\alpha_m r_1\right)\mathrm{e}^{\mathrm{i}n\theta_1}+\frac{\alpha_m^2}{2}\left[\frac{h^2}{24}\left(\frac{1}{\kappa}-1\right)+\delta_m-\frac{h^2}{24}\frac{1-2\kappa}{\kappa}\left(\alpha_m^2-k_1^2\right)\delta_m\right]$$
$$\times\left[\frac{\eta_2^2}{\rho_2^2}\frac{\Omega'(\eta_2)}{\overline{\Omega'(\eta_2)}}\mathrm{H}_{n-2}^{(1)}(\alpha_m r_1)\mathrm{e}^{\mathrm{i}(n-2)\theta_1}+\frac{\bar{\eta}_2^2}{\rho_2^2}\frac{\overline{\Omega'(\eta_2)}}{\Omega'(\eta_2)}\mathrm{H}_{n+2}^{(1)}(\alpha_m r_1)\mathrm{e}^{\mathrm{i}(n+2)\theta_1}\right]\quad(m=1,2)$$

$$K_{43}^n=\frac{k_2^2}{2}\mathrm{i}\left[\frac{\eta_2^2}{\rho_2^2}\frac{\Omega'(\eta_2)}{\overline{\Omega'(\eta_2)}}\mathrm{K}_{n-2}(k_2 r_1)\mathrm{e}^{\mathrm{i}(n-2)\theta_1}-\frac{\bar{\eta}_2^2}{\rho_2^2}\frac{\overline{\Omega'(\eta_2)}}{\Omega'(\eta_2)}\mathrm{K}_{n+2}(k_2 r_1)\mathrm{e}^{\mathrm{i}(n+2)\theta_1}\right]$$

$$K_{4m}^n=\left\{\frac{1-2\kappa}{\kappa}-\frac{1-\kappa}{\kappa}\left[1+\frac{h^2}{24}\left(\alpha_{m-3}^2-k_2^2\right)\right]\alpha_{m-3}^2\delta_{m-3}+\frac{h^2}{24}\left(\frac{2-3\kappa}{\kappa}\alpha_{m-3}^2-\frac{1-2\kappa}{\kappa}k_2^2\right)\right\}$$
$$\times\mathrm{H}_n^{(1)}\left(\alpha_{m-3}r_2\right)\mathrm{e}^{\mathrm{i}n\theta_2}+\frac{\alpha_{m-3}^2}{2}\left[\frac{h^2}{24}\left(\frac{1}{\kappa}-1\right)+\delta_{m-3}-\frac{h^2}{24}\frac{1-2\kappa}{\kappa}\left(\alpha_{m-3}^2-k_1^2\right)\delta_{m-3}\right]$$

$$\times\left[\frac{\eta_2^2}{\rho_2^2}\frac{\Omega'(\eta_2)}{\overline{\Omega'(\eta_2)}}\mathrm{H}_{n-2}^{(1)}(\alpha_{m-3}r_2)\mathrm{e}^{\mathrm{i}(n-2)\theta_2}+\frac{\bar{\eta}_2^2}{\rho_2^2}\frac{\overline{\Omega'(\eta_2)}}{\Omega'(\eta_2)}\mathrm{H}_{n+2}^{(1)}(\alpha_{m-3}r_2)\mathrm{e}^{\mathrm{i}(n+2)\theta_2}\right]\quad(m=4,5)$$

$$K_{46}^n=\frac{k_2^2}{2}\mathrm{i}\left[\frac{\eta_2^2}{\rho_2^2}\frac{\Omega'(\eta_2)}{\overline{\Omega'(\eta_2)}}\mathrm{K}_{n-2}(k_2r_2)\mathrm{e}^{\mathrm{i}(n-2)\theta_2}-\frac{\bar{\eta}_2^2}{\rho_2^2}\frac{\overline{\Omega'(\eta_2)}}{\Omega'(\eta_2)}\mathrm{K}_{n+2}(k_2r_2)\mathrm{e}^{\mathrm{i}(n+2)\theta_2}\right]$$

$$K_{5m}^n=\frac{\alpha_m^2}{2}\left[\frac{\eta_2^2}{\rho_2^2}\frac{\Omega'(\eta_2)}{\overline{\Omega'(\eta_2)}}\mathrm{H}_{n-2}^{(1)}(\alpha_m r_1)\mathrm{e}^{\mathrm{i}(n-2)\theta_1}-\frac{\bar{\eta}_2^2}{\rho_2^2}\frac{\overline{\Omega'(\eta_2)}}{\Omega'(\eta_2)}\mathrm{H}_{n+2}^{(1)}(\alpha_m r_1)\mathrm{e}^{\mathrm{i}(n+2)\theta_1}\right]$$
$$\times\left[\frac{h^2}{24}\left(\frac{1}{\kappa}-1\right)+\delta_m-\frac{h^2}{24}\frac{1-2\kappa}{\kappa}\left(\alpha_m^2-k_1^2\right)\delta_m\right]\quad(m=1,2)$$

$$K_{53}^n=\frac{k_2^2}{2}\mathrm{i}\left[\frac{\eta_2^2}{\rho_2^2}\frac{\Omega'(\eta_2)}{\overline{\Omega'(\eta_2)}}\mathrm{K}_{n-2}(k_2r_1)\mathrm{e}^{\mathrm{i}(n-2)\theta_1}+\frac{\bar{\eta}_2^2}{\rho_2^2}\frac{\overline{\Omega'(\eta_2)}}{\Omega'(\eta_2)}\mathrm{K}_{n+2}(k_2r_1)\mathrm{e}^{\mathrm{i}(n+2)\theta_1}\right]$$

$$K_{5m}^n=\frac{\alpha_{m-3}^2}{2}\left[\frac{\eta_2^2}{\rho_2^2}\frac{\Omega'(\eta_2)}{\overline{\Omega'(\eta_2)}}\mathrm{H}_{n-2}^{(1)}(\alpha_{m-3}r_2)\mathrm{e}^{\mathrm{i}(n-2)\theta_2}-\frac{\bar{\eta}_2^2}{\rho_2^2}\frac{\overline{\Omega'(\eta_2)}}{\Omega'(\eta_2)}\mathrm{H}_{n+2}^{(1)}(\alpha_{m-3}r_2)\mathrm{e}^{\mathrm{i}(n+2)\theta_2}\right]$$
$$\times\left[\frac{h^2}{24}\left(\frac{1}{\kappa}-1\right)+\delta_{m-3}-\frac{h^2}{24}\frac{1-2\kappa}{\kappa}\left(\alpha_{m-3}^2-k_1^2\right)\delta_{m-3}\right]\qquad(m=4,5)$$

$$K_{56}^n=\frac{k_2^2}{2}\mathrm{i}\left[\frac{\eta_2^2}{\rho_2^2}\frac{\Omega'(\eta_2)}{\overline{\Omega'(\eta_2)}}\mathrm{K}_{n-2}(k_2r_2)\mathrm{e}^{\mathrm{i}(n-2)\theta_2}+\frac{\bar{\eta}_2^2}{\rho_2^2}\frac{\overline{\Omega'(\eta_2)}}{\Omega'(\eta_2)}\mathrm{K}_{n+2}(k_2r_2)\mathrm{e}^{\mathrm{i}(n+2)\theta_2}\right]$$

$$K_{6m}^n=\alpha_m\left[\frac{1}{\kappa}\left(\alpha_m^2-k_1^2\right)\delta_m-\frac{1-2\kappa}{\kappa}\right]\left[\frac{\eta_2}{\rho_2}\frac{\Omega'(\eta_2)}{|\Omega'(\eta_2)|}\mathrm{H}_{n-1}^{(1)}(\alpha_m r_1)\mathrm{e}^{\mathrm{i}(n-1)\theta_1}\right.$$
$$\left.-\frac{\bar{\eta}_2}{\rho_2}\frac{\overline{\Omega'(\eta_2)}}{|\Omega'(\eta_2)|}\mathrm{H}_{n+1}^{(1)}(\alpha_m r_1)\mathrm{e}^{\mathrm{i}(n+1)\theta_1}\right]\quad(m=1,2)$$

$$K_{6m}^n=\alpha_{m-3}\left[\frac{1}{\kappa}\left(\alpha_{m-3}^2-k_1^2\right)\delta_{m-3}-\frac{1-2\kappa}{\kappa}\right]\left[\frac{\eta_2}{\rho_2}\frac{\Omega'(\eta_2)}{|\Omega'(\eta_2)|}\mathrm{H}_{n-1}^{(1)}(\alpha_{m-3}r_2)\mathrm{e}^{\mathrm{i}(n-1)\theta_2}\right.$$
$$\left.-\frac{\bar{\eta}_2}{\rho_2}\frac{\overline{\Omega'(\eta_2)}}{|\Omega'(\eta_2)|}\mathrm{H}_{n+1}^{(1)}(\alpha_{m-3}r_2)\mathrm{e}^{\mathrm{i}(n+1)\theta_2}\right]\quad(m=4,5)$$

$$K_1=-\left\{\frac{1-2\kappa}{\kappa}-\frac{1-\kappa}{\kappa}\left[1+\frac{h^2}{24}\left(\alpha_1^2-k_2^2\right)\right]\alpha_1^2\delta_1+\frac{h^2}{24}\left(\frac{2-3\kappa}{\kappa}\alpha_1^2-\frac{1-2\kappa}{\kappa}k_2^2\right)\right.$$
$$\left.-\alpha_1^2\left[\frac{h^2}{24}\left(\frac{1}{\kappa}-1\right)+\delta_1-\frac{h^2}{24}\frac{1-2\kappa}{\kappa}\left(\alpha_1^2-k_1^2\right)\delta_1\right]\mathrm{Re}\left(\frac{\eta_1}{\overline{\eta_1}}\frac{\Omega'(\eta_1)}{\overline{\Omega'(\eta_1)}}\right)\right\}E_0\exp\left(\mathrm{i}\alpha_1\mathrm{Re}\left(\Omega(\eta_1)\right)\right)$$

$$K_2=\mathrm{i}\alpha_1^2\left[\frac{h^2}{24}\left(\frac{1}{\kappa}-1\right)+\delta_1-\frac{h^2}{24}\frac{1-2\kappa}{\kappa}\left(\alpha_1^2-k_1^2\right)\delta_1\right]\mathrm{Im}\left(\frac{\eta}{\overline{\eta}}\frac{\Omega'(\eta_1)}{\overline{\Omega'(\eta_1)}}\right)E_0\exp\left(\mathrm{i}\alpha_1\mathrm{Re}\left(\Omega(\eta_1)\right)\right)$$

$$K_3=-2\,\mathrm{i}\alpha_1\left[\frac{1}{\kappa}\left(\alpha_m^2-k_1^2\right)\delta_m-\frac{1-2\kappa}{\kappa}\right]\mathrm{Re}\left(\frac{\eta_1}{\rho}\frac{\Omega'(\eta_1)}{|\Omega'(\eta_1)|}\right)E_0\exp\left(\mathrm{i}\alpha_1\mathrm{Re}\left(\Omega(\eta_1)\right)\right)$$

$$K_4=-\left\{\frac{1-2\kappa}{\kappa}-\frac{1-\kappa}{\kappa}\left[1+\frac{h^2}{24}\left(\alpha_1^2-k_2^2\right)\right]\alpha_1^2\delta_1+\frac{h^2}{24}\left(\frac{2-3\kappa}{\kappa}\alpha_1^2-\frac{1-2\kappa}{\kappa}k_2^2\right)\right.$$
$$\left.-\alpha_1^2\left[\frac{h^2}{24}\left(\frac{1}{\kappa}-1\right)+\delta_1-\frac{h^2}{24}\frac{1-2\kappa}{\kappa}\left(\alpha_1^2-k_1^2\right)\delta_1\right]\mathrm{Re}\left(\frac{\eta_2}{\overline{\eta_2}}\frac{\Omega'(\eta_2)}{\overline{\Omega'(\eta_2)}}\right)\right\}E_0\exp\left(\mathrm{i}\alpha_1\mathrm{Re}\left(\Omega(\eta_2)\right)\right)$$

$$K_5=\mathrm{i}\alpha_1^2\left[\frac{h^2}{24}\left(\frac{1}{\kappa}-1\right)+\delta_1-\frac{h^2}{24}\frac{1-2\kappa}{\kappa}\left(\alpha_1^2-k_1^2\right)\delta_1\right]\mathrm{Im}\left(\frac{\eta_2}{\overline{\eta_2}}\frac{\Omega'(\eta_2)}{\overline{\Omega'(\eta_2)}}\right)E_0\exp\left(\mathrm{i}\alpha_1\mathrm{Re}\left(\Omega(\eta_2)\right)\right)$$

$$K_6=-2\mathrm{i}\alpha_1\left[\frac{1}{\kappa}\left(\alpha_m^2-k_1^2\right)\delta_m-\frac{1-2\kappa}{\kappa}\right]\mathrm{Re}\left(\frac{\eta_2}{\rho}\frac{\Omega'(\eta_2)}{|\Omega'(\eta_2)|}\right)\times E_0\exp\left(\mathrm{i}\alpha_1\mathrm{Re}\left(\Omega(\eta_2)\right)\right)$$

$$\eta_1=\exp\left(\mathrm{i}a\theta_1\right),\quad r_2=\sqrt{a^2+d^2+2ad\sin\theta_1},\quad\theta_2=\arccos\left(\frac{a\cos\theta_1}{r_2}\right)$$

$$\eta_2=\exp\left(\mathrm{i}a\theta_2\right),\quad r_1=\sqrt{a^2+d^2-2ad\sin\theta_2},\quad\theta_1=-\arccos\left(\frac{a\cos\theta_2}{r_1}\right)$$